

Mapping of mechanical properties of cast iron melts using non-destructive structuroscopy

J. Dočekal^a, B. Skrbek^{a,*}, I. Tomáš^b

^a Department of Material Science, Technical University of Liberec, Studentská 2, CZ-46117 Liberec I, Czech Republic

^b Institute of Physics of the ASCR, v. v. i., Na Slovance 2, CZ-182 21 Praha 8, Czech Republic

*Corresponding author. E-mail address: skrbek@motory.tedom.cz

Received 08.02.2008; accepted in revised form 17.03.2008

Abstract

The contribution is focused on mapping of mechanical properties using methods of non-destructive structuroscopy of cast irons, which are a result of research at TU of Liberec and Institute of Physics of ASCR. Investigated samples become from melts of FOCAM s.r.o Olomouc Foundry shop. It compares data of mechanical properties obtained using ultrasound method with data from magnetic spot method and MAT. These are interpreted by mathematic models applicable in practice. In the following it concerns to derivation of loading tensile curve method, which can be used to obtain yield and fatigue strength limits even for cast irons with flake graphite. In spite of promising results reported by literature the experiments are bothered with error. This method can be applied to structure checking both before casting and at vendor inspection of castings.

Keywords: Cast iron; Non-destructive testing; Mechanical properties.

1. Introduction

The research activity of Department of Material Science of Faculty of Mechanical Engineering solves among others determination of ultimate states of cast irons loading. The presented structuroscopy methods [1] enable to measure mechanical properties of cast iron castings without failure (or grinding of surface in the measurement place) effectively with high productivity. Their application finds validation namely at mass production of safety parts of traffic vehicles made from cast iron castings. The successful appropriation of these methods requires knowledge of statistics and patience naturally. In the frame of experiment can be introduced an example of pro-and-noc of exploitation possibility of limited set of cast iron samples for prediction of relation between mechanical and physical

properties of castings from compact cast irons of one foundry shop.

2. Ultrasound methods

Transmissivity of acoustic waves through material decreases with damping of matrix matter and namely with quantity and size of internal discontinuities. As a discontinuity can be considered inclusions with considerably different resistance Z against matrix [2].

$$Z=c \times \rho \quad [\text{MPa/s}] \quad (1)$$

Amount and quantity of reflectance R increases with increasing difference of acoustic resistances Z_m and Z_g from boundary back

$$R = (Z_g - Z_m) / (Z_g + Z_m) \quad (2)$$

For steel matrix of cast iron is valid $Z_m = 5,92 \times 7,2 = 46,2$ MPa/s, for graphite is approximately valid $Z_g = 2 \times 2 = 4$ MPa/s. Boundary matrix - graphite reflects $R = 80,5\%$ of pressure of acoustic wave. Direct propagation of acoustic wave through cast iron is after several reflections from graphite formations spent and dispersed. Size of path of acoustic wave through matrix depends on labyrinth of graphite formation. With increasing weakening of matrix by graphite formation increases the value of acoustic path L_u in comparison with direct path (thickness of wall) L . Sound velocity c_L sink that way.

$$c_L = c_{L0} \times L / L_u = 5920 \times L / L_u \text{ [m/s]} \quad (3)$$

c_{L0} ... sound velocity of cast iron steel matrix. If in rapidly cooled part of casting metastable crystallization of eutectics occurs (it means that carbon instead of deposition in the form of graphite binds to iron forming carbide Fe_3C and suspends as a hard ledeburite) occurs less obstacles against propagation of acoustic wave and for this reason sound velocity value increases with increasing amount of ledeburite in the structure.

Amplitude damping of acoustic oscillations α increases markedly if wavelength λ approaches to size l of graphite formations [6]

$$\alpha = k_a \times l \times (c_L / \lambda)^2 \text{ [dB/mm]} \quad (4)$$

Value $\alpha = 0,05$ for steels enables sound through even one-metre wall thicknesses. Graphite increases damping markedly. For cast iron with flake graphite reaches values of greater order which very restricts faults detection. Most of castings can be characterized intrinsic resonance f_r , which is the function of elasticity modulus E (it describes shape of graphite), specific weight (amount of graphite) and geometry slenderness H/D . Frequency f_r can be found usually in the audible extent [7]

$$f_r = k_f \times (E/\rho)^{0,5} \times D/H^2 \text{ [Hz]} \quad (5)$$

E value depends directly on size of sound velocity c_L thus on shape and amount of graphite.

$$c_L = \{(E/\rho) \times (1 - \mu) / [(1 + \mu) \times (1 - 2 \times \mu)]\}^{0,5} \text{ [m/s]} \quad (6)$$

By modification (6) can obtain simplified expression where L is true wall thickness and L_u wall measured by ultrasound

$$E = (K \times L / L_u)^2 \text{ [MPa]} \quad (7)$$

3. Impulsion method of magnetic spot

This method is focused on local measurement of remanent magnetism H_m with ballistic (impulse) method of magnetization.

In steel the in the same way oriented atoms are concentrated in domains, that create any subgrains in the grains of structure (Figure 1). By polarization using external magnetic field occurs growth of domains by displacement so called Bloch zones and by polarization consistent with external magnetic field or occurs jump change of polarization by so called Barkhausen jumps (source of Barkhausen noise). After disappearing external magnetic field H_0 not all domains return to original state. Remanent polarization I_r is created. Magnetized place has his own magnetic field with intensity H_r . The reversible changes are prevented by atoms of ferromagnetics bond in molecules and atomic tension, lattice faults. For this reason structure components, which contains iron carbide, martensite, numerous dislocations and grain boundaries shows high value of remanent polarization I_r .

$$H_r = H_0 - N \times I_r / \mu \text{ [A/m]} \quad (8)$$

Demagnetizing factor N characterizes both external and structure geometry circumstances of ferromagnetics boundary.

The tested site of product is effected by impulsion magnetic field with intensity H_0 . The shape of current impulse conducted to attached to power coil, eventually exactly defined sequency of them defines flow of parasite Foucault currents (they can be properly used to suppression of negative influences of N) and structur-selective sensitivity of method. The methods used in Russian and in Czech republic differs essentially in magnetization characteristics and by it in the aim of applications. The sensor of H_r can be Hallova or Försterova probe. The contribution dH_{ri} of single grain of ferromagnetics to resulting value H_r depends on shielding action m and their distance t_i from probe

$$H_r = \sum m \times t_i \times dH_{ri} \quad (9)$$

With increasing depth S penetration of magnetic field sinks the influence of single grains on H_r . In practice upto $t = 12$ mm. In thinner walls so pulse energy concentrates to less volume of grains. H_r value upto value L_{kri} increases after experimentally determined model.

$$H_{rL} = H_{rL12} \times (81 \times L^{-3} + 1) \quad (10)$$

Iron alloys (steels and cast irons) create the spectrum of most widespread structural materials. Ferromagnetic properties can be ordered to their overwhelming majority. The knowledge of mechanical properties in critically loaded site of exposed parts dominate over necessity of integral information about choiced mechanical property. For these reasons has local magnetic microscopy significant position in the spectrum of remainder methods. It found application widening in the form of impulsion magnetic checking mainly in Russian and in Bohemia.

High checking productivity with targeted high sensitivity to checked structur parameter enables checking of state of recrystallizing of cold-worked product - anisotropy, measurement of mechanical properties after annealing, different method of measurement after hardening and tempering. Elimination of influence of putting off - measurement through layers upto 3 mm thick. Devices in manufacturing lines of flat products. In western Europe is for this region of materials used exclusively ET

method. But alternative eddy currents describe more surface section of work pieces. For products in the form of worked semiproducts and castings with untreated surfaces is more acceptable local magnetic structuroscopy.

4. Mapping of mechanical properties of castings from FOCAM s.r.o. Olomouc melts

To obtain data of mechanical properties using ultrasound and magnetic impulse method were used samples made from Y-block melts of FOCAM Ltd. Their chemical composition see Table 1.

Table 1.
Chemical composition of cast iron castings from FOCAM s.r.o. Olomouc

Melt No.	C (%)	Mn (%)	Si (%)	S (%)	Cu (%)	Cr (%)	Mg (%)	P (%)
1	3,41	0,25	2,2	0,014	1	0,06	0,045	0,02
2	3,73	0,24	1,6	0,013	0,04	0,06	0,051	0,02
3	3,3	0,25	2,45	0,016	0,04	0,05	0,046	0,02
4	3,46	0,26	2,12	0,014	0,05	0,07	0,019	0,02
5	3,63	0,26	2,44	0,022	1,01	0,04	0,016	0,03

From following metallographic sections was determined matrix and shape of graphite. (Table 2, Figure 1).

Table 2.
Types of cast iron

Melt No.	matrix	graphite	rate of pearlite	rate of graphite
1	P94,P1,Pd0,5	GVI 6/7, (GV)	0,93	0,14
2	F30,P1 35, Cm35	GVI6/5 95%,GIII	0,4	0,12
3	P15-20, P1	GIII 85%, GVI	0,2	0,17
4	P40-50%, P1	GIII 75-80%,GVI	0,34	0,13
5	F90 P10, P1	GVI7/6,90%,GIII	0,04	0,09

Presented content 1% Cu of melt 5 don't correspond to recieved ferrite matrix in as-cast state

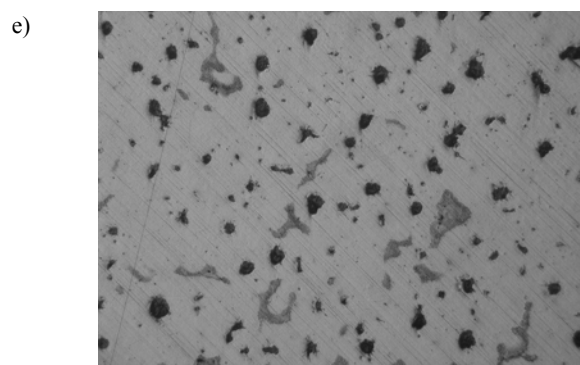
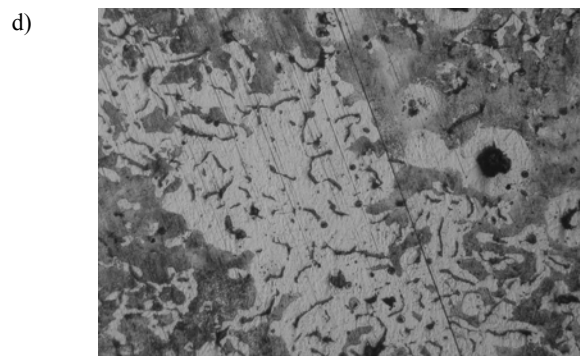
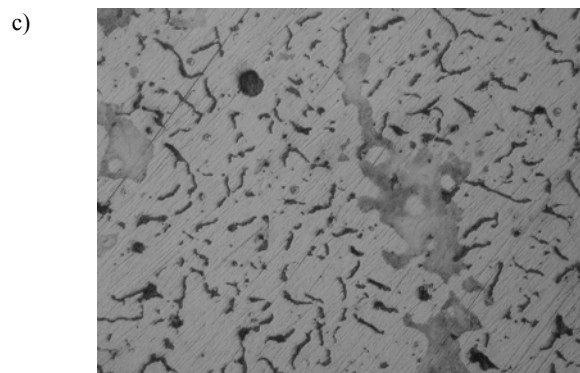
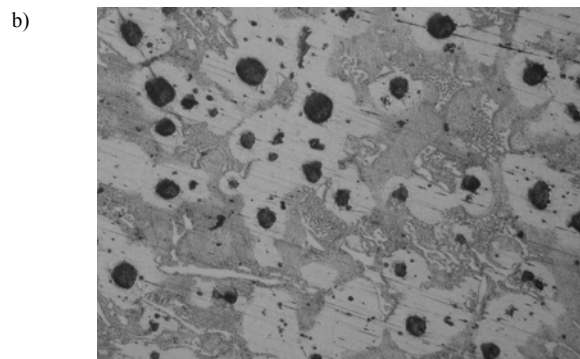
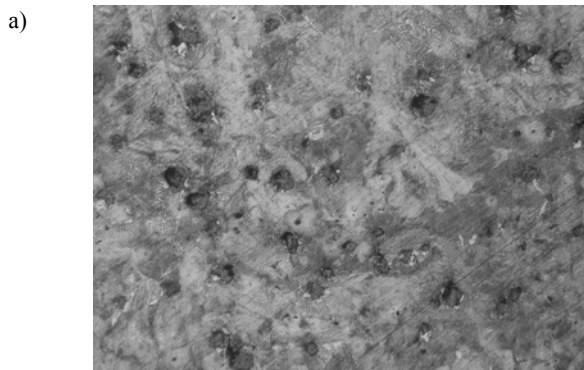


Fig. 1. Metallography sections of single melts (magnified 100x, Nital etched)

a) Melt No. 1, b) Melt No. 2, c) Melt No. 3, d) Melt No. 4, e) Melt No. 5

Table 3.

Values of properties obtained by mechanical tests

Bar	HB	R _{p0,2}	R _m	A5 %	E-graf
[marking]	[5/750kp]	[MPa]	[MPa]	[%]	[GPa]
1Y1-4a	246	475	825	9,23	206,82
1Y1-4b	215,17	476	824	10,94	174,86
2Y1-1a	171	448	800	8,34	178,19
2Y1-1b	177,5	356	550	2,39	162,24
3Y1-1a	151,67	230	314	7,73	153,77
3Y1-1b	172,83	230	318	6,92	149,41
4Y1-2a	166,17	Praha	Praha	Praha	Praha
4Y1-2b	164,5	323	418	3,33	141,71
5Y1-1a	161,33	290	427	18,41	167,79
5Y1-1b	159	287	410	8,11	179,29
1Y2-3a	228,33	386	804	8,99	189,26
1Y2-3b	233	443	800	8,34	193,97
2Y2-6a	158,33	bez dat	bez dat	bez dat	bez dat
2Y2-6b	160,83	263	462	7,95	147,74
3Y2-3a	153	230	298	5,77	157,77
3Y2-3b	149,67	230	299	6,04	149,16
4Y2-1a	161,17	318	408	3,37	119,82
4Y2-1b	154	Praha	Praha	Praha	Praha
5Y2-3a	166,33	291	432	20	216,69
5Y2-3b	162,33	291	427	18,62	166,41

4.1. Ultrasound measurement

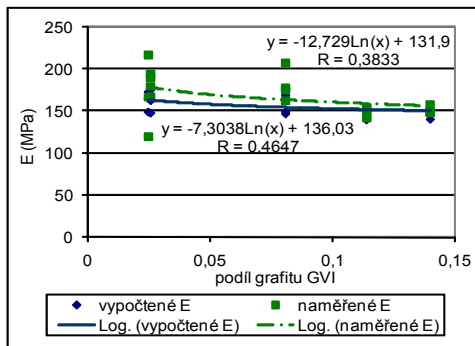


Fig. 2. Dependence of sound velocity v_L on fraction of graphite in structure

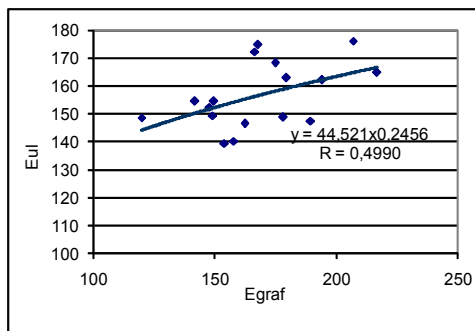


Fig. 3. Relation of velocity v_L and fracture of only GVI graphite in structure

Ultrasound measurement was made using instrument DIO562 with probe SEB2 on samples taken from a Y1-blocks of single melts. By measurement on cylindrical bars were obtained constants K for calculation of elasticity modulus [6].

$$E_{oUL} = (K \cdot L / L_u)^2 \text{ [GPa]} \quad (11)$$

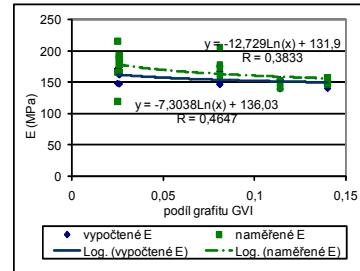


Fig. 4. Relation between elasticity modulus from tensile test record E_{gr} and from measurement by ultrasound E_{ul} fracture GVI graphite in structure

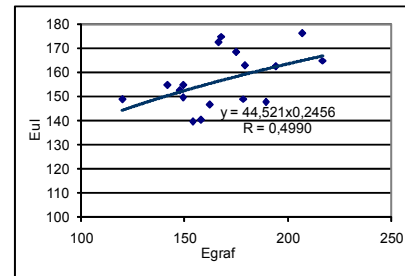


Fig. 5. Dependence of initial elasticity modulus obtained from tensile test record E_{gr} and from measurement by ultrasound E_{ul} .

4.2. Impulsion magnetic measurement

Values obtained by DOMENA B3 instrument are given in Table 4.

Measurement was performed partly on rectangular semiproducts taken from Y-blocks ($M_{Polotovar}$) and on bars made from these semiproducts ($M_{Na\text{ průměru}}$). For measurement on bars was used non-metallic preparative to adjustment of probe in order to keep comparability of obtained data.

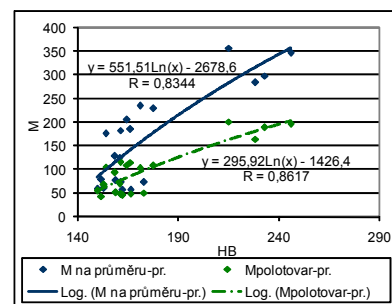


Fig. 6. Dependence of M value on HB hardness

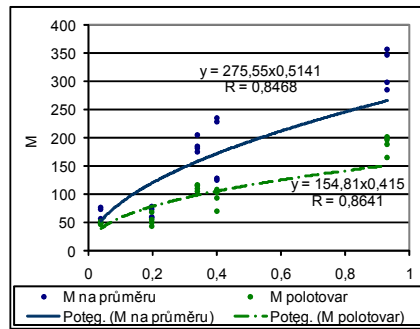


Fig. 7. Dependence of M value on pearlite amount

Table 4.

Values obtained by ultrasound on cylindrical semiproduct bars for tensile test

[marking]	L [mm]	L _U [mm]	d [mm]	G [g]	τ [mm]	v _L [m/s]	μ [l]	E ₀ [GPa]	ρ [g/cm ³]	K [l]
1A1	147,9	153,23	28,5	680,4	24,28	5714,077	0,315135	167,1699	7,211351	423,5988
1A2	147,55	153,05	28,5	679,4	23,2	5707,259	0,297039	176,0865	7,217833	435,2684
1A3	146,45	151,85	28,95	690,6	23,4	5709,476	0,294304	176,2047	7,163912	435,2454
1A4	148	153,5	28,45	677,5	23,1	5707,883	0,296041	176,1928	7,201007	435,3522
1A5	146,15	151,4	28,7	682,5	23,35	5714,716	0,297346	176,4162	7,218555	435,1072
1A6	146	151,3	26,9	595,6	21,6	5712,624	0,291801	177,9213	7,178067	437,1194
2A1	149,45	156,1	28,6	688,4	23,5	5667,803	0,298014	172,0498	7,170065	433,2455
2A2	147,9	154,65	27,6	634,5	23,3	5661,61	0,30823	166,7124	7,1706	426,9389
2A3	Z	Z	Z	Z	Z	#####	#####	#####	#####	#####
2A4	146,9	y	27,3	616,3	1	#####	#####	#####	7,167295	#####
2A5	Z	Z	Z	Z	Z	#####	#####	#####	#####	#####
2A6	149,6	156,1	29,1	709,5	23,85	5673,491	0,29739	171,7487	7,130911	432,4322
2A7	146	151,9	27,5	627,9	22,2	5690,059	0,292375	177,7914	7,240732	438,6926
2A8	Z	Z	Z	Z	Z	#####	#####	#####	#####	#####
2A9	145,25	152,1	27,9	641,9	23,8	5653,386	0,311639	165,8399	7,228581	426,4397
3A1	146,1	161,6	27,9	632,1	22,07	5352,178	0,255603	167,1368	7,076807	452,1965
3A2	146,7	163	26,8	588,2	22,45	5328	0,280081	157,8011	7,107805	441,3799
3A3	146,4	162,1	28	633,8	23,07	5346,626	0,274257	159,3249	7,030809	441,9608
3A4	147,4	163,4	28,3	655,3	24,3	5340,318	0,291657	153,1536	7,067731	433,8285
3A5	147,7	163,94	28	639	23,63	5333,561	0,283774	154,9263	7,026103	436,8849
3A6	147,3	163,55	27,5	624,1	24,1	5331,801	0,299351	150,9166	7,133395	431,3366
4A1	148,9	168	28,8	684,5	24,74	5246,952	0,284362	150,3721	7,056738	437,5203
4A2	149,1	167	29	690,6	24,4	5285,461	0,278485	153,7846	7,012343	439,2333
4A3	148,8	167,1	29	690,5	23,9	5271,67	0,26791	156,9575	7,025463	444,9022
4A4	149,4	167,8	28,9	691,7	24,75	5270,846	0,285	151,5332	7,058001	437,2152
4A5	147,5	166,4	29	684,2	23,95	5247,596	0,266752	155,8528	7,022719	445,3675
4A6	149,6	168	28,9	690,7	24,25	5271,619	0,276109	154,3982	7,038375	441,2643
5A1	147,85	153,2	27,2	614,4	21,8	5713,264	0,291066	177,645	7,151585	436,7309
5A2	144,55	149,73	28,35	649	22,77	5715,194	0,292092	176,3237	7,112638	434,9567
5A3	148,7	151,15	28,15	657,7	25,5	5824,042	0,342609	154,9728	7,106738	400,152
5A4	146,95	152,13	27,2	600,5	21,9	5718,425	0,293343	173,9618	7,032598	431,7896
5A5	145,55	150,83	28,4	651	22,71	5712,763	0,290075	175,8049	7,060611	434,5012
5A6	147,2	152,6	28,95	688,5	23,1	5710,511	0,289003	177,2768	7,105738	436,4883
Average values										436,6

Table 6.

Values obtained by impulsion magnetic method If partial dependences for samples Y1 and Y2 are created, pearlite evaluation by eye and using Lucia SW is made, even at linear regression substantially more close relations shall be obtained! Initial values are shown by restored table.

M ₁ Na průměru	Bar	M ₂ Na průměru	M ₁ Polotovár	M ₂ Polotovár	M ₃ Polotovár
[w/m ²]	[marking]	[w/m ²]	[w/m ²]	[w/m ²]	[w/m ²]
361	1Y1-4a	335	204	190	185
363	1Y1-4b	352	208,5	195	190
243	2Y1-1a	229	105,5	100,25	99
229	2Y1-1b	230	111,5	105,5	104
78,3	3Y1-1a	80,4	44,55	43,05	43,45
72,9	3Y1-1b	74,3	52,4	49,8	49
203	4Y1-2a	169	116,5	114,5	109
225	4Y1-2b	188	110,5	108,5	108
76,3	5Y1-1a	70,9	50,55	47,05	44,1
78,3	5Y1-1b	77	53,25	51,3	50,55
279	1Y2-3a	292	169	160,5	158
293	1Y2-3b	305	195,5	183	177,5
133	2Y2-6a	126	95,15	92,5	93,45
134	2Y2-6b	119	71,25	68,75	68,7
61,9	3Y2-3a	61,2	70,95	66,85	66,45
57,8	3Y2-3b	59,8	56,25	55	53,35
188	4Y2-1a	178	118,5	114,5	111
183	4Y2-1b	170	107,5	104,5	101
59,1	5Y2-3a	56,4	49,4	48,5	47,5
55,7	5Y2-3b	59,8	46,8	45,85	48,1

Table 7.

Metallography evaluation

Melt	1	2	3	4	5
%P eye	94	35	17	45	10
%P Lucia	93	40	20	34	4
Y1M1 mid	206	108	49	113,5	51,8
Y2M1 mid	183	79	63	113	48

$$\text{Poko} = \text{Y1M1x0,515-14} \quad R=0,99 \quad (11)$$

$$\text{Pluc} = \text{Y1M1x0,514-16} \quad R=0,97 \quad (12)$$

$$\text{Poko} = \text{Y2M1x0,613-19} \quad R=0,992 \quad \text{P100} = 226\text{M1} \\ \text{P0} = 32\text{M1} \quad (13)$$

$$\text{Pluc} = \text{Y2M1x0,6-20} \quad R=0,956 \quad (14)$$

Magnetic measurement give more close results with visual estimation. Metallography analysis was made on 5 Y1bars, though even corellation of Y2 values alone gives very close dependence to %P. By mixing of Y1M and Y2M values into one set the regression coefficient R sinks markedly. Substantial role plays her shape coefficient – function part of block Y1 is very near and thin (for the front of probe 21mm DOMENA B3) in comparison with Y2 block.

4.3. Mathematic models for non-destructive measurement R_m, R_{p(0,2)}

I this part are introduced models obtained by measurement on samples from foundry shop FOCAM s.r.o., which can be applied on determination of R_m, R_{p(0,2)} using nondestructive methods. It is about dependence R_m, R_{p(0,2)} on hardness HB and M value.

$$R_m = f(\text{HB}) = 1133,4 \cdot \ln(\text{HB}) - 5360,3 \quad R=0,9565 \quad (15)$$

$$R_p = f(\text{HB}) = 456,9 \cdot \ln(\text{HB}) - 20384 \quad R=0,8723 \quad (16)$$

$$R_m = f(M_{\text{na průměru}}) = 58,58 \cdot (M_{\text{na průměru}})^{0,423} \quad R=0,8444 \quad (17)$$

$$R_p = f(M_{\text{na průměru}}) = 66,57 \cdot (M_{\text{na průměru}})^{0,318} \quad R=0,8883 \quad (18)$$

$$R_m = f(M_{\text{polotovár}}) = 296,64 \cdot \ln(M_{\text{polotovár}}) - 816,43 \quad R=0,8650 \quad (19)$$

$$R_p = f(M_{\text{polotovár}}) = 135,05 \cdot \ln(M_{\text{polotovár}}) - 275,22 \quad R=0,8908 \quad (20)$$

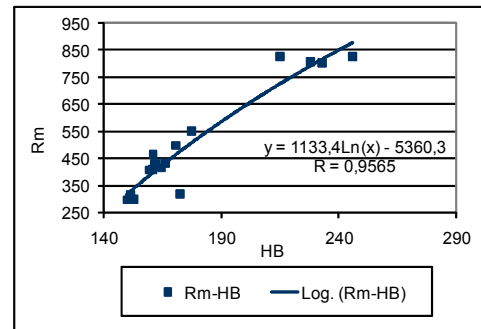


Fig. 8. Dependence R_m on HB hardness

For three parameter dependence of strength R_m (R_p) on M, v_L (eventually HB, v_L) can be applied relations:

$$R_m = 8,54 \times (L/L_u)^{5,257} \times \text{HB}^{0,86} \quad (21)$$

$$R_p = 9,3 \times (L/L_u)^3 \times \text{HB}^{0,756} \quad (22)$$

$$A = 132000 \times (L/L_u)^{13} \times \text{HB}^{-1,635} \quad (23)$$

4.4. Derivation of tensile characteristics

Tensile characteristic of cast irons with flake graphite has generally non-linear course (Hookian law is not valid). After Exner [5] and another works, lately Jech [8] has derivative course typical shape determining searched limits R_E σ_I σ_{II}. But our experiments showed difficulties at measurement and treatment of results recorded by laser extensometer by derivation.

5. Discussion

5.1. Ultrasound measurement

From diagrams of dependence of sound velocity on relative content of graphite in matrix is obvious how great influence has shape of graphite on obtained data. While at application of relative content of graphite without difference of shape shows only minimum dependence on sound velocity, so at relative content only GVI graphite is dependence marked with confidence value $R=0,947$.

At the dependence of elasticity modulus on relative graphite content the shape of graphite has not so fundamental effect on this dependence such as at previous relation both for elasticity modulus from tensile test record E_{gr} and for modulus measured using ultrasound E_{ul} .

5.2. Impulsion magnetic measurement

From both diagrams in chapter impulsion magnetic measurement is obvious that measured values are influenced by not only shape of graphite (which is not considered here) but also the shape of measured sample. The shape influences the size of obtained values, but at application of suitable preparative for keeping of probe is the course of dependence nearly the same. But the regression curve is both in the case of hardness and in the case of relative pearlite content more adjoining to values measured on semiproduct. It only confirms the importance of surface state at ultrasound measurement. Magnetic measurement influences significantly overcritical shape of measured place. If this state is eliminated, the relation of magnetism M values to pearlite fraction or to hardness is very close. The pearlite fraction can be measured with great accuracy!

5.3 Mathematic models

On mathematic models (15 - 22) as well is expressed surface shape effect and amount and shape of graphite in the structure. It sounds interesting that M value is more adjacent to yield strength R_p then to strength R_m , but it is not valid for dependence of strength R_m on hardness HB , where the adjacency is just opposite. For mathematic model R_m on HB is reliability value $R=0,9565$. The abovementioned tridimensional dependence (21) and (22) seems to be most suitable for description of strength R_m or yield strength R_p .

6. Conclusions

Initial material for successful appropriation of non-destructive structuroscopy methods is set of casting of standard bars (e.g. Y

blocks, bars 30) with satisfactorily wide extent of mechanical properties. On the pouring surface are performed magnetic measurements, on semiproducts of bars measurements of HB and by ultrasound. Measurement with magnetic spot method are acceptable for strong curved surfaces as well. The testing bars are made from semiproducts and tensile tests are performed. Of course, all dependencies and mathematic models are influenced by little number of measurements, where instead of tens should be numbered in order of hundreds but nevertheless from this results can be found out dependencies important for more easy interpretation and application of NDT methods such as ultrasound and impulsion magnetic method. The main benefit is possibility of rapid reliable operational checking by measuring on only grit-blasted surfaces of castings. For thin-walled casting is ultrasound measurement incorrect. In the frame of cooperation with FzU AVČR is performed research of only magnetic measurement [4]. The both methods simultaneously are used through relations (2; 13; 14; 15) at measuring on untreated surfaces of castings by combined structuroscopy TELIT [7].

Acknowledgements

This contribution was created with support of project AVČR 1QS100100508 and research plan MSM 4674788501.

References

- [1] B. Skrbek, Nedestruktivní materiálová diagnostika litin: kandidátská disertační práce, Jablonec 1988.
- [2] B. Skrbek, I. Tomas, Impulzní magnetická strukturoskopie plochých ocelových výrobků. In METAL 2003, 12th Int. Conf. Ostrava : TANGER s.r.o., CD ROM proceedings, paper 48.
- [3] B. Skrbek, Mechanické vlastnosti litin v odlitcích s ohledem na tloušťku stěn a průtočnost kovu a přilíhých zkušebních tělesech In 4. Int. Metallurgy Symp. METAL '95. Ostrava : TANGER, 1995, s. 164 – 168.
- [4] I. Tomáš, B. Skrbek, O. Stupakov, L. Vokurka, Local adaptive and standard magnetic structuroscopy of cast iron. New Trends in Physics, Proceedings of the conference. Brno, University of Technology, 2004, p. 93-94. ISBN 80-7355-024-5.
- [5] J. Exner, J. Čech, Hodnocení vlastností litin podle tahových deformačních charakteristik. In Slévárenská ročenka 1993, s.45-51.
- [6] J. Obráz, J. Zkoušení materiálu ultrazvukem. Praha : SNTL, 1989. ISBN 80-03-00097-1.
- [7] B. Skrbek, Výběr a zpracování dat experimentálně změřených v SKS v kampaních r. 2006 : Projekt MPO F1 – 1M/001 Report No. 74-40SKS.
- [8] M. Jech, I.Nova, I. Nováková, Sledování pevnostních charakteristik litiny s lupinkovým a kuličkovým grafitem. Slévárenství , 2006, no.9, p. 340-345.